Biochemical Journal (2018) **475** 1597–1610
https://doi.org/10.1042/BCJ20180035

PORTLAND PRESS

Research Article

Nucleic acid-induced potentiation of matrix metalloproteinase-9 enzymatic activity

Tyler Duellman, Xi Chen, Rie Wakamiya and Jay Yang

Department of Anesthesiology, University of Wisconsin, School of Medicine and Public Health, Madison, WI 53705, U.S.A.

Correspondence: Jay Yang (jyang75@wisc.edu)

Matrix metalloproteinases (MMPs) play varied roles in normal biology and diseases where, depending on the context, both inhibition and enhancement of the enzymatic activity may be beneficial. However, there are very few reports of positive modulators of MMP activity. We report that polynucleotides, including single-stranded DNA, RNA, and even double-stranded DNA, bind to and enhance the enzymatic activity of MMP9. This enhancement of MMP9 catalytic activity is not shared by biologically active polycationic molecules suggesting nonspecific charge screening as an unlikely mechanism. Deletion construct and MMP1, 2, and 3 studies suggest that the type-II fibronectin repeat domains of the enzyme appear to play a role in mediating the nucleotide potentiation of MMP9 activity. Single-stranded DNA enhances nerve growth factor-induced MMP9-dependent neurite extension in pheochromocytoma 12 cells providing evidence for potential biological significance of the nucleotide-mediated allosteric enhancement of the catalytic activity.

Introduction

Matrix metalloproteinases (MMPs) constitute a family of enzymes with a wide role in normal biology and diseases. The initially described limited role of MMP in shaping the extracellular matrix has now expanded to include intracellular substrates in addition to the better studied extracellular substrates that make up the extracellular matrix. Overactivity of MMP has been associated with many disease-specific conditions, such as plaque destabilization leading to stroke, weakening of the extracellular matrix support leading to aortic aneurysms, enhancing cancer cells to access the circulation leading to distant metastasis, and many more. As such, much effort has gone into the discovery of MMP inhibitors with specificity acting only on the desired target members of the MMP family. However, MMPs also play a role in normal biology such as wound healing [1], cardiac remodeling after injury [2], and possibly consolidation of memory through regulation of synaptic plasticity [3,4] where an increase in MMP activity could potentially be beneficial. The discovery of a small molecule enhancing specific MMP activities would contribute toward a better understanding the biological processes benefiting from increased MMP activity and such positive modulators could be therapeutically useful.

In contrast with the abundant literature on MMP inhibitors, those that describe enhancement of MMP activity are limited. Yamamoto et al. [5] broadly summarize three mechanisms of allosteric enhancement of MMP activity by: (1) acceleration of proenzyme activation to the active form, (2) localization of active MMP on the cell surface by binding to cell surface proteins or extracellular matrix proteins, and (3) pharmacokinetic accumulation of MMP availability by modulating endocytotic clearance of the active enzyme. Emonard and Hornebeck [6] reported that insoluble elastin enhanced MMP2 activity by accelerating the enzyme activation or the conversion of the inactive pro-form to the catalytically active form. Elastin, gelatin, and type IV collagen bind to the fibronectin type-II (FNII) repeat domains of MMP2. This is consistent with the structural analysis of MMP2 which indicates that the side chain of Phe37 in the pro-peptide inserts into the hydrophobic pocket of the FNII domain mimicking the binding of gelatin to the FNII domain [7]. A further study confirmed

Received: 12 January 2018
Revised: 11 April 2018
Accepted: 12 April 2018

Accepted Manuscript online: 13 April 2018
Version of Record published: 9 May 2018

Biochemical Journal (2018) 475 1597–1610
https://doi.org/10.1042/BCJ20180035

that the elastin acceleration of MMP9 activation occurred not only by the more typical proteolytic cleavage of the N-terminus pro-peptide protecting the catalytic domain but also through an allosteric conformational change of the protein allowing activation without cleavage [8]. None of the proposed mechanisms that enhance MMP activity, including the acceleration of activation, are true enhancers of the enzymatic activity, but rather pharmacokinetic enhancers in nature resulting in greater availability of the activated enzyme without increasing the specific enzyme activity.

We initiated this project to identify DNA aptamers capable of enhancing MMP9 enzymatic activity acting allosterically. Nucleotides, including single-stranded DNA, have been shown to assume specific three-dimentional folded structures capable of binding to a target protein with great specificity and high affinity. DNA aptamers binding to various proteases have been reported (reviewed in Dupont et al. [9]), but all the reported aptamers inhibit the proteases; however, there is no reason why a similar strategy should not be able to identify a DNA aptamer that enhances the protease activity. DNA aptamers with such desirable properties can be selected from a starting library of very large diversity through repeated rounds of binding and amplification by a process termed systematic evolution of ligands by exponential enrichment (SELEX) originally described to select for a thrombin-binding aptamer that inhibits clot formation [10]. We specifically sought DNA aptamers binding to a site on the MMP9 protein outside the catalytic domain by using pro-MMP9 as our target protein where the conserved catalytic domain is covered by the pro-domain of the protein. Allosteric sites show less homology between different MMPs allowing, in theory, identification of a more specific modulator of MMP9 distinguishing between the closely related MMP family members [11].

We report a surprising observation that not only single-stranded DNA but also nucleotides, including RNA, enhance MMP9 activity. This positive modulatory effect of polynucleotides on MMP9 activity is not shared with other typical polyanionic molecules, but appears to be a specific effect of the polynucleotides on the FNII repeat domain of the enzyme.

Materials and methods

Generation of molecular constructs

Wild-type human MMP9 cDNA (BC006093, Image Clone MGC: 12688) was PCR-amplified to remove the stop codon and incorporate a unique in-frame Mlu I restriction enzyme sited at the 3′-terminus and ligated into the PCR Blunt (Invitrogen, Carlsbad, CA). Analogous 3′ mCherry-tagged constructs for human MMP1, 2, and 3 were created starting from clones MHS6278-20283008, MHS1011-59214, and MHS6278-202856824, respectively (Dharmacon GE Healthcare, Lafayette, CO). The PCR product was sequence confirmed and subcloned into the pCI/neo vector (Promega, Madison, WI) upstream and in-frame of an mCherry fluorescent tag cDNA where the start ATG was replaced with a Mlu I sequence. The standard two-step PCR method was used for amplifying various DNA fragments required, and the appropriate fragments were ligated for creating the deletion and tagged constructs. Further details can be found in Duellman et al. [12]. The primers used for PCR amplifications required for creating various constructs are listed in Supplementary Table S1.

Cell culture

Human embryonic kidney (HEK) 293 cells (#CRL-1572, ATCC, Manassas, VA) were grown in Dulbecco's Modification of Eagle's Medium (DMEM; Mediatech, Inc., Manassas, VA) with 4.5 g/l glucose, L-glutamine, sodium pyruvate, and supplemented with 10% heat-inactivated fetal bovine serum (FBS) (Mediatech, Inc.), 100 U/ml penicillin (Mediatech, Inc.), and 0.1 mg/ml streptomycin (Mediatech, Inc.) in a 5% CO_2-humidified incubator at 37°C. PC12 rat pheochromocytoma cells (#CRL-1721, ATCC) were grown in the above medium, except supplemented with 10% horse serum and 5% FBS. SF9 insect cells (#11496015, Life Technologies, Carlsbad, CA) were grown in SF900 II (#10902096, Life Technologies) supplemented with penicillin/streptomycin antibiotics on a shaking platform in a room air incubator at 18°C.

Clustered regularly interspaced short palindromic repeat-mediated genomic knockout

N-terminal rat MMP9 (NM) was searched for guide RNA target sites using the online software (crispr.mit.edu/guides). Pairs of oligonucleotides targeting the four highest scoring guide RNA sites along with sgBlank containing no insert were annealed and ligated into the lentiCRISPRv2 (clustered regularly interspaced short palindromic repeat) vector (Addgene #52961) after vector digestion with BsmBI following the Zhang Lab Lentiviral

CRISPR Toolbox protocol (https://www.addgene.org/static/data/plasmids/52/52961/52961-attachment_B3xTwla0bkYD.pdf). Lentivirus was rescued by co-transfection of HEK293 cells with the lentiCRISPRv2 harboring the target gRNA site with the helper psPAX2 and pVSVG plasmids (Addgene #12260 and #12259). Three days post-transfection, the medium containing the lentivirus was harvested, passed through a 45-μm filter, and added directly to the PC12 cell culture medium. Four days post-infection, selection with puromycin (2 μg/ml) was initiated. Cell colonies were picked after islands of surviving cells became visible and further expanded in the puromycin medium. Of the four gRNA target sites explored, ccagcgccagccgacttatg targeting nucleotides 66–85 (top strand) of rat MMP9 cDNA (NM031055) resulted in the PC12 knockout cell line.

Fluorescence polarization

In a total reaction volume of 30 μl, 10 nM of FAM-labeled oligonucleotides was added with different concentrations of purified MMP9 (Enzo Life Sciences) or ovalbumin (OVA) in binding buffer (20 mM HEPES, pH 6.5, 40 mM NaCl, 20 mM $CaCl_2$, and 100 nM $ZnCl_2$). The mixture was added to a 384-well plate and incubated at room temperature for 15 min. Fluorescence polarization was quantified at room temperature using a PHERAstar multimode plate reader (BMG LABTECH, Offenburg, Germany).

Agarose electrophoretic mobility shift assay

Protein/oligonucleotide samples were incubated at room temperature for 15 min and then separated in a 1% agarose gel containing 0.5 μg/ml ethidium bromide at 20 V/cm for 15 min in 1× TAE buffer (40 mM Tris–acetate, 2 mM EDTA, pH 8.3). Gels were imaged using Quality One software (Bio-Rad) with a ChemiDoc XRS+ Molecular Imager (Bio-Rad). Images were processed using Photoshop.

Surface plasmon resonance

The nucleotide interaction with C-terminus His-tagged MMP9-mCherry fusion protein or a negative-control mCherry alone was performed using a gold nanoparticle-based localized SPR (surface plasmon resonance; Open SPR, Nicoya Life Systems, Kitchner, ON, Canada). The target protein was isolated from the supernatant of SF9 cells infected with baculovirus designed to express the MMP9.mCherry.TEV.His fusion protein using a Ni-affinity column (NTA Spin Column, Qiagen) (Supplementary Figure S1) and the approximate protein concentration estimated from the mCherry fluorescence of the fusion protein [13]. The enzymatic activity of the APMA (*p*-aminophenylmercuric acetate)-activated eluted MMP.mCherry.TEV.His was confirmed by the fluorometric activity assay. Baculovirus was created by first creating a modified pFastbac 1 vector where nucleotides encoding TEV-His (amino acids ENLYFQGHHHHHH) were inserted into the Xho I and Hind III restriction enzyme sites by annealing two single-stranded oligonucleotides. A PCR-amplified mCherry sequence flanked by Mlu I and Xho I was subcloned into the pFastbac 1-TEV-His to create a pFastbac 1-mCherry-TEV-His vector. The cDNA of interest was subcloned into this vector and the Bac-to-Bac Expression System (#10359016, Life Technologies) used to create a recombinant bacmid and the baculovirus particle rescued according to the procedure described in the kit. Note that the constructs had an N-terminal calreticulin secretory sequence so that the expressed proteins were efficiently secreted into the culture media. The His-tagged protein was bound to the nitrilotriacetic acid (NTA) sensor chip according to the protocol from Nicoya Life Systems and after confirming stable baseline, ssDNA (single-stranded DNA) of varying concentrations in the running buffer passed over the sensor chip. Control experiments passing anti-MMP9 or anti-mCherry antibody over the sensor chip confirmed the proper presence of the bound MMP.mCherry.TEV.His protein. The resulting spectrogram was analyzed with Trace Drawer Kinetic Data Analysis v.1.6.1 (Nicoya Life Systems) using a one-to-one model (i.e. one monovalent ligand binding to one target) with only baseline subtraction of control spectrogram with no ligand correction applied.

In vitro poly-(ADP-ribose)-polymerase 1-1 degradation assay

With 1 mM APMA, 10 ng of human pro-MMP9 (Enzo Life Sciences, Farmingdale, NY) was activated at 37°C for 2 h. To the activated MMP9, 100 ng of human PARP-1 [poly-(ADP-ribose)-polymerase 1; Sino Biological, Beijing, China] was added with or without increasing concentrations of 40-mer oligonucleotides in assay buffer (25 mM Tris–HCl, 100 mM NaCl, 2.5 mM $CaCl_2$, 750 nM $ZnCl_2$, and 0.025% Brij-35, pH 7.0) for 2 ½ h at 37°C. Reactions were stopped in RIPA buffer containing a protease inhibitor cocktail (Bio-Rad).

Biochemical Journal (2018) 475 1597–1610
https://doi.org/10.1042/BCJ20180035

Fluorometric MMP-9 enzymatic activity assay

The SensoLyte 520 MMP-9 Assay Kit (Ana Spec, Inc., #71155, Fremont, CA) was used to determine the enzymatic activity of MMPs with and without oligonucleotides. Purified MMP protein was added at the indicated concentrations in MMP Dilution Buffer (50 mM Tris–HCl, 200 mM NaCl, 5 mM $CaCl_2$, 1 μM $ZnCl_2$, 0.05% Brij-35, and 0.05% NaAzide, pH 7.0) with the addition of the indicated concentrations of oligonucleotides. Hundred microliters of hMMP9/oligonucleotide samples were supplemented with 1 μM $ZnCl_2$ and 2 mM APMA, mixed, added to a black 96-well plate, and incubated at 37°C for 1 h. APMA was omitted from the reaction when assaying for the catalytic domain — MMP9 since preactivation was not required. After incubation, a final concentration of 20 μM of the fluorogenic substrate (Enzo Life Sciences) in 100 μl of 2× assay buffer (100 mM HEPES, 20 mM $CaCl_2$, and 0.1% Brij-35, pH 7.0) was added to the activated MMP protein and reaction kinetics were quantified using a Synergy 2 microplate reader (BioTek, Inc., Winooski, VT) with an excitation wavelength/bandwidth of 360/40 and an emission wavelength/bandwidth of 460/40 at 37°C for 1 ½ h. Unless otherwise indicated, the final concentration of MMP9 protein was 2 nM with variable concentrations of ssDNA in the final assay reaction.

Western blot

Cell culture media and cell pellets lysed in RIPA buffer (10 mM Tris–Cl, pH 7.5, 50 mM NaCl, 1 mM sodium orthovanadate, 30 mM sodium pyrophosphate, 50 mM NaF, 1% NP40, 0.1% SDS, 1 mM phenylmethylsulfonyl fluoride, 1% Triton X-100, and 0.5% sodium deoxycholate) were collected for analysis. Twenty micrograms of cell lysate and an equal volume of cell media were loaded in 10% SDS–PAGE gels [14]. Samples were run and transferred onto 0.45 μm nitrocellulose membranes that were blocked using 5% milk and washed in TBS-T (Tris-buffered saline with 0.1% Triton X-100). Membranes were probed with appropriate antibodies and imaged using the Quality One software (Bio-Rad) with a ChemiDoc XRS+ Molecular Imager (Bio-Rad). Densitometric quantitation of Western blots was performed using Image Lab 4.1 software (Bio-Rad).

Gelatin zymography

A 10% polyacrylamide gel supplemented with 0.1% gelatin was loaded with cell lysate and separated by electrophoresis. The enzyme in the gel was renatured for 1 h in Triton X-100 (2.5%, v/v), developed overnight at 37°C in a buffer (50 mM Tris, 200 mM NaCl, 50 mM $CaCl_2$, 5 μM $ZnCl_2$, and 0.02% Brij-35, pH 7.5), stained (0.5% Coomassie blue in 30% methanol and 10% acetic acid) for 2 h at room temperature, and destained (30% methanol and 10% acetic acid) until the bands were visible. Gels were placed on a white light box and images were captured on a Chemi-Doc XRS+ Molecular Imager (Bio-Rad). The molecular mass marker was not visible on the zymography gel, and a parallel gel loaded with the marker was run and the marker lane excised in Photo Shop.

Neurite image analysis

PC12 cells were plated on collagen-coated cell culture plates in DMEM supplemented with 10% horse serum and 5% FBS. Adherent cells were stimulated with NGF (nerve growth factor; 50 ng/ml) in 1% (horse serum)/0.5% fetal bovine serum for 4 days and fixed with 4% PFA (paraformaldehyde). The fixed cells were immunocytochemically stained with an anti-β-III-tubulin antibody (1 : 1000, #339, Abcam, Cambridge, U.K.) to identify the neurites and counterstained with Hoechst reagent (2 μg/ml) to identify the cell nuclei. Ten random fields of both β-III-tubulin and Hoechst images were captured under 200× magnification, and the images were processed in ImageJ using the NeuriteTracer plugin [15]. The number of nuclei and neurite pixel density were quantified from the images.

Oligonucleotide pull-down assay by SELEX

The procedure follows as described by Murphy et al. [16] with modifications. The bait protein was MMP9-mCherry-His expressed in baculovirus as described under the SPR method. The bait protein bound to magnetic Ni-NTA slurry was washed with 1 ml of PBST three times and the eluted protein was resuspended to ~5 pmol/μl and stored at 4°C. Ten-fold excess (1 nmol) N40 single-stranded DNA library (#O-32001, TriLink Biotech, San Diego, CA) was added to 100 pmol bait protein in 10 ml of PBST supplemented with 0.1 μg/ml BSA and 0.1 μg/ml tRNA, rotated for 30 min at room temperature, and the aptamer bound to the bait protein isolated by a magnetic pull-down. The beads were washed with 1 ml of PBST three times and the aptamer-bait

protein complex eluted from the NTA beads in 10 μl of elution buffer (500 mM imidazole and 20 mM Tris, pH 7.5). A 5′ FAM-tagged forward primer and a 3′ biotin-tagged reverse primer targeting the common flanking sequences of the library were used to PCR amplify the pulled-down aptamer. The double-stranded (ds) PCR product was bound to the streptavidin beads (80 μl of PCR product, 20 μl of 5 M NaCl, and 100 μl of washed streptavidin-magnetic beads). After washing in 1 ml of PBST three times, the FAM-labeled positive strand bound to the beads was released by elution in 50 μl of 50 mM NaOH, immediately neutralized by the addition of 40 μl of binding buffer and 10 μl of phosphate buffer (pH 7.5), and used as the aptamer input for the next round of the pull-down assay. Fluorescence measurement of the FAM-tagged aptamer pool enabled monitoring of the enrichment of the aptamer during progression of the SELEX rounds (Supplementary Figure S1). Negative SELEX rounds with mCherry-His bait protein and isolating the unbound aptamer fraction were introduced after rounds 4 and 8 of positive SELEX rounds.

Other reagents

4-Aminophenylmercuric acetate (APMA) (#A9563) and Gelatin Type-A (#G8150) were purchased from Sigma–Aldrich (St. Louis, MO). Fluorogenic MMP substrate (#BML-P128), catalytic domain-recombinant MMP-9 (#BML-SE360), purified MMP-2 (#BML-SE503), and purified MMP-9 (#BML-504) were purchased from Enzo Life Sciences. Note that the purchased purified MMPs, both catalytic domain only and full length, were not 6×His-tagged. Polyanionic molecules chondroitin sulfate (C4384), laminarin (L9634), fucoidan (F8190), suramin (S2671), lipopolysaccharide (L2262), and heparin (H4784) were purchased from Sigma–Aldrich.

Statistical analysis

Data are plotted as mean ± SEM unless otherwise noted in the figure legends, $N = 3$–12 biological replicates were obtained for each assay with two experimental replicate measurements per assay. Statistically significant differences in the mean values were defined as $P < 0.05$ by *t*-test or ANOVA, as appropriate. Calculated *P*-values are denoted as **** <0.001, *** <0.005, ** <0.01, and * <0.05.

Results

A SELEX pull-down experiment was initiated to identify biotinylated 40-mer ssDNA binding to the MMP9-mCherry protein target immobilized on a streptavidin-magnetic bead (Supplementary Figure S1). The bound DNA aptamers were eluted and PCR-amplified to generate a pool of DNA aptamers for the subsequent rounds of SELEX. An agarose gel electrophoresis of the amplified DNA aptamer after round 10 of SELEX showing abundant PCR-amplified product binding to the target MMP9 protein with little binding to the negative-control mCherry is shown in Figure 1A. The bound ssDNA aptamer appeared to show convergence after 10 rounds of positive selection against MMP9-mCherry interleaved with two rounds of negative selection against mCherry alone. This 40-mer ssDNA identified by SELEX, we call A3, showed binding to catalytic core-MMP9 (cMMP9) by the electrophoretic mobility shift assay (Figure 1B), fluorescence polarization assay (Figure 1C), and SPR (Figure 1E,F). The calculated binding parameters from the SPR data were association rate constant $k_a = 8.7E+4 \pm 6.1E+2$ $(1/(M*s))$, a dissociation rate constant $k_d = 1.16\ E-3 \pm 1.0\ E-5$ $(1/s)$ with an equilibrium dissociation constant $(k_d/k_a) = 1.34E-8 \pm 2.1\ E-10$ (M). Further exploration with a 40-mer RNA by fluorescence polarization assay, however, demonstrated a similar apparently specific binding of RNA to the MMP9 target comparable to the evolved and selected A3 ssDNA with no evidence of binding to the negative-control OVA (Figure 1D). Subsequent experiments with non-selected (scrambled) 40-mer ssDNA also confirmed that the binding of ssDNA to MMP9 was not sequence-specific (Supplementary Figure S2A). Very large dsDNA from isolated gDNA or sheared gDNA with a much smaller distributed fragment size enhanced MMP9 activity in a manner indistinguishable from the well-defined 40-mer dsDNA created by annealing two complimentary strands of ssDNA (Supplementary Figure S2B,C). These results suggested a surprising nucleotide binding to MMP9 shared by ssDNA, dsDNA, and RNA.

We characterized the effects of polynucleotides on MMP9 activity by a fluorescent substrate cleavage assay using a synthetic MMP substrate peptide and a more physiological DQ-gelatin substrate where the kinetic increase in the fluorescent signal served as a readout of the enzymatic activity. The ssDNA A3 greatly increased the MMP9 enzymatic activity (Figure 2A). There was no difference in enzymatic kinetics or ssDNA-induced enzymatic potentiation between the synthetic MMP9 substrate peptide and DQ-gelatin, so the MMP substrate peptide was used in the remainder of the *in vitro* enzymatic assays (Supplementary Figure S3). Consistent with

Biochemical Journal (2018) **475** 1597–1610
https://doi.org/10.1042/BCJ20180035

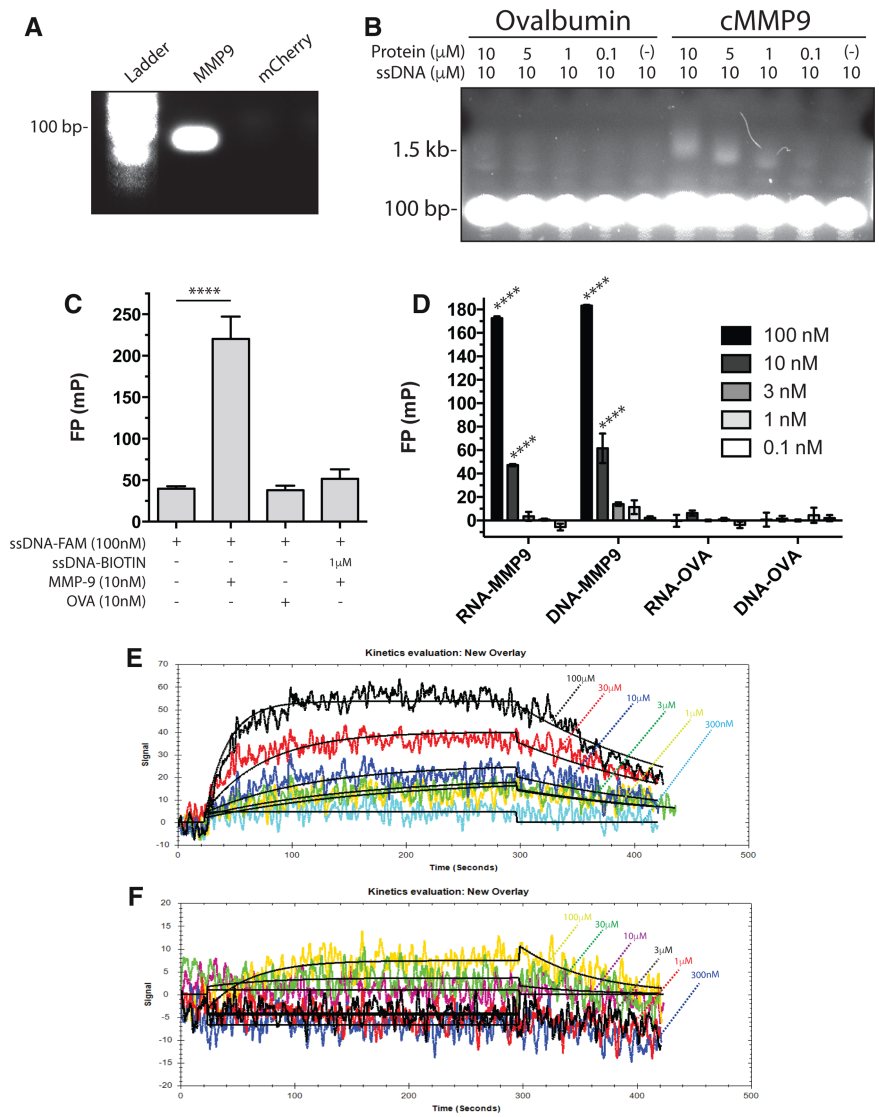

Figure 1. Interaction of DNA and RNA oligomers with MMP9.

(**A**) PCR amplification of DNA oligomers co-purified with either MMP9.mCherry.His or mCherry.His. (**B**) Increasing concentrations of purified MMP9 catalytic domain or OVA were incubated with ssDNA oligomers. Protein : DNA interactions were analyzed by an electrophoretic mobility shift on an agarose gel. (**C**) Fluorescence polarization of FAM-labeled ssDNA incubated with MMP9 (full length) or OVA. Saturating levels of ssDNA-Biotin were used for fluorescence polarization competition of ssDNA-FAM. (**D**) Fluorescence polarization of increasing concentrations of 40-mer RNA or 40-mer ssDNA incubated with MMP9 or OVA. Dose–SPR response of increasing 40-mer ssDNA oligomer bound to MMP9.mCherry.His (**E**) or mCherry (**F**).His-labeled NTA-Ni-SPR flow cells. The traces are for 100, 30, 10, 3, 1, and 0.3 μM ssDNA.

the fluorescent polarization data indicating RNA binding to MMP9, ssDNA, RNA, and even 40-mer dsDNA created by annealing two complementary ssDNA all increased the MMP9 enzymatic activity (Figure 2B). We explored the effect of ssDNA length on enzymatic activity increase and found that ssDNA down to ∼4-mer enhanced the MMP9 activity, while 2-mer and single nucleotides failed to do so (Figure 2C). Given this observation that short ssDNA enhanced MMP9 activity and the fact that the surface of the MMP9 protein has pockets of positively charged areas (Figure 2D), we explored whether the modulation of enzymatic activity was shared by other polyanionic molecules. A range of polyanionic molecules with reported biological activity, such as chondroitin sulfate, laminarin, fucoidan, suramin, LPS, and heparin, failed to modulate the MMP9 enzymatic activity within the 5–500 μg/ml concentration range examined. To minimize the chances of an enzymatic

Biochemical Journal (2018) **475** 1597–1610
https://doi.org/10.1042/BCJ20180035

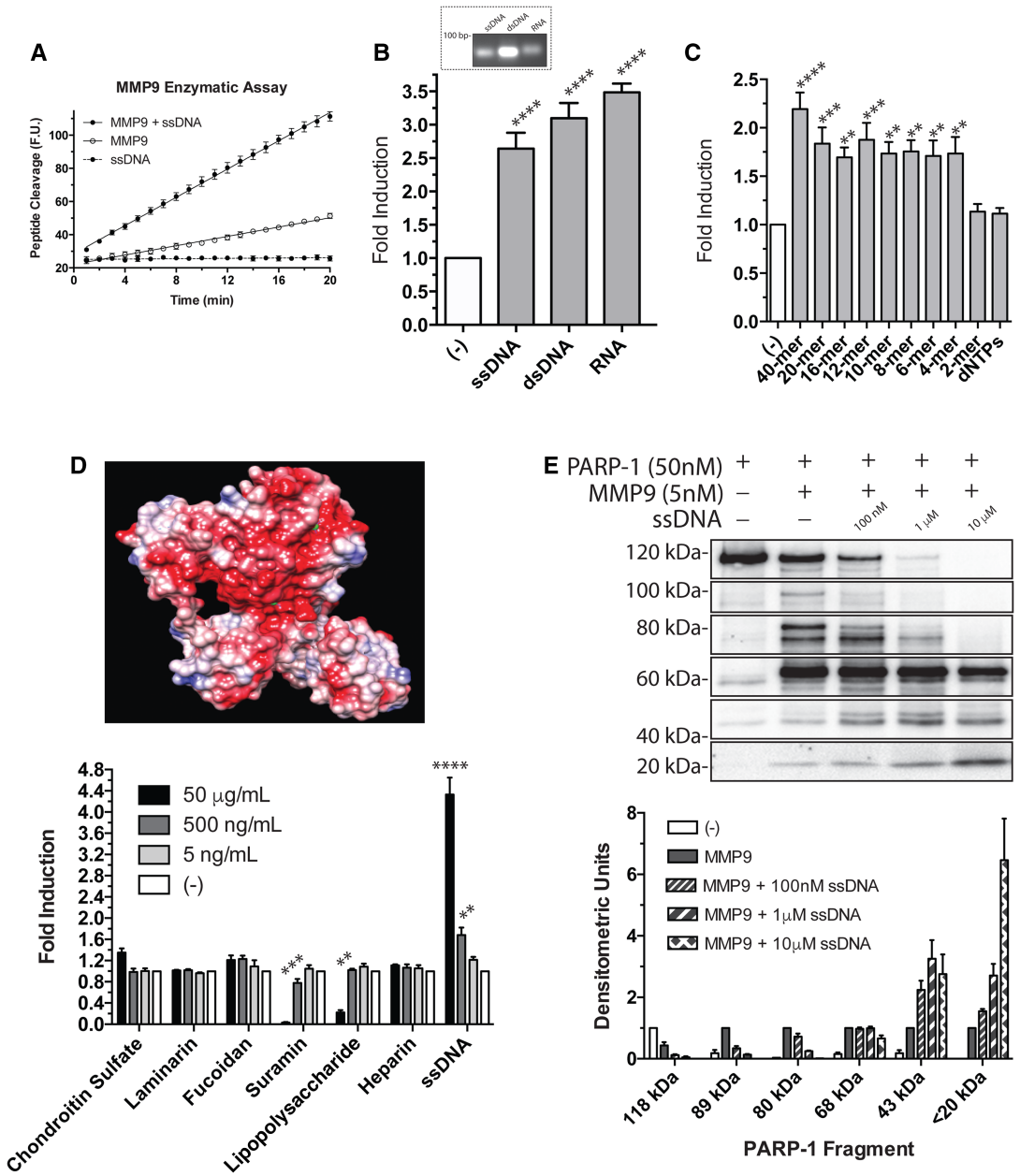

Figure 2. Nucleic acid potentiation of MMP9 enzymatic activity.

(**A**) Real-time analysis of cleaved fluorescent-labeled MMP substrate of MMP9 only (open circle, solid line), DNA oligomer only (black circle, dashed line), or MMP9 and 40-mer DNA (black circle, solid line). (**B**) Fold induction of enzymatic activity above MMP9 only with 40-mer ssDNA, 40-mer dsDNA, or 40-mer RNA (all at 1 μM). dsDNA was confirmed by ethidium bromide staining on agarose gel (inset), ssDNA and RNA showed low-level ethidium bromide intercalation due to some intramolecular ds character. (**C**) Fold induction over MMP9 alone of different length DNA oligomers or dNTPs. All nucleotides were present at 1 μM in the activity assay reaction. (**D**, top) A surface electrostatic potential of C-terminus truncated MMP9 crystal structure (PDB: 1l6j) displayed using PyMOL. Red indicates positive and blue indicates negative charges. (Bottom) Fold induction of MMP9 enzymatic activity with increasing concentrations of different polyanionic molecules over MMP9 activity alone. (**E**) Western blot detection of MMP9-induced PARP-1 cleavage fragments using a polyclonal antibody (top). Densitometric analysis of the different cleavage fragments of PARP-1 alone (white), PARP-1 with MMP9 (gray), and PARP-1 with MMP9 and increasing concentrations of ssDNA (gray with dashes).

Biochemical Journal (2018) **475** 1597–1610
https://doi.org/10.1042/BCJ20180035

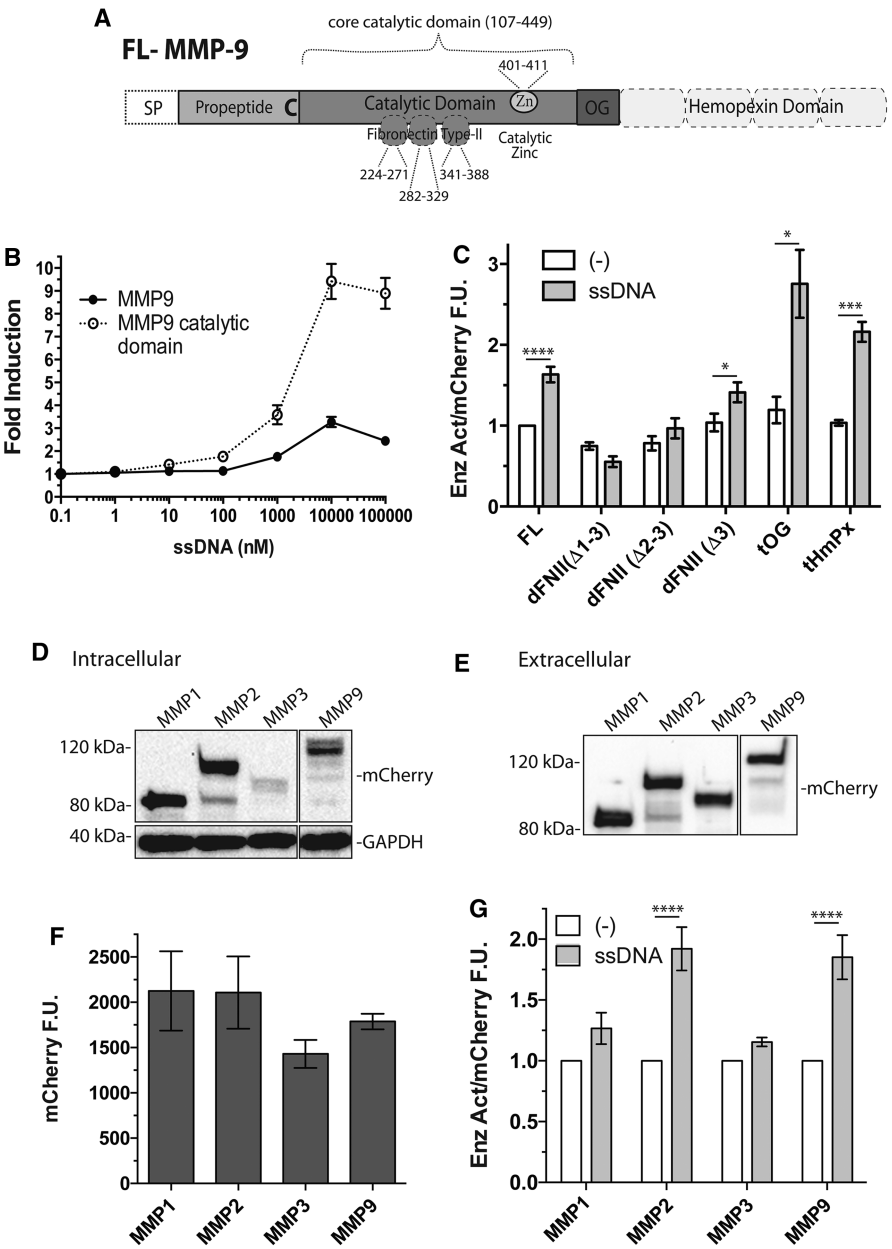

Figure 3. Allosteric interaction domain of MMP9 and oligonucleotide.

(**A**) Cartoon illustration of the domain structure of MMP9. Amino acid residues are indicated for the tripartite FNII repeat followed by the enzymatic cleft co-ordinated with the catalytic zinc molecule within the catalytic domain. Signal peptide, SP; cysteine switch, C; O-glycosylation domain, OG. (**B**) Dose–response of enzymatic potentiation for the purified full-length (closed circle, solid line) or purified catalytic domain (open circle, dashed line) of MMP9. The catalytic domain spans amino acid residues 107–449 as indicated in the cartoon above. (**C**) Enzymatic activity of overexpressed MMP9.mCherry without (white) or with 1 μM ssDNA (gray) of full-length (FL) control or different truncation/deletion mutants. mCherry fluorescence is used to normalize MMP9 input. Hemopexin domain truncation, tHmPx; O-glycosylation domain and hemopexin domain truncation, tOG; triple fibronectin-domain deletion, ΔFNII (Δ1–3); double fibronectin-domain deletion, ΔFNII (Δ2–3); single fibronectin-domain deletion, ΔFNII (Δ3). Domain 1 contains residues 224–271, domain 2 contains residues 282–329, and domain 3 contains residues 341–388. Western blots of mCherry-tagged MMP1, MMP2, MMP3, or MMP9 (no 6xHis tag) expressed in transfected HEK293 cells detected by blotting with an anti-mCherry antibody. Cellular lysate (**D**) or culture media (**E**) show expressed proteins of the expected molecular mass. (**F**) Relative expressed protein amounts in the culture media by direct measurement of mCherry fluorescence. (**G**) MMP activity assay normalized by mCherry fluorescence without (white) or with (gray) 1 μM ssDNA.

activity assay-dependent erroneous conclusion, we examined the effect of ssDNA on PARP cleavage as an alternative assay. PARP is a substrate for MMP9 and the enzymatic activity cleaves the PARP protein into several fragments ranging 20–100 kDa [17,18]. MMP9 cleaved the PARP protein and ssDNA increased the intensity of cleaved products in a concentration-dependent manner (Figure 2E), confirming the increase in the MMP9 enzymatic activity by ssDNA by this assay as well.

ssDNA enhanced the enzymatic activity of AMPA-activated full-length MMP9 in a concentration-dependent manner. ssDNA by itself did not induce activity of non-pre-activated full-length MMP9 (Supplementary Figure S4), suggesting that activation either by cleavage of the pro-peptide or through a conformational change without cleavage of the protective pro-peptide, as has been shown for insoluble gelatin, is not how ssDNA acts on MMP9. MMP9 has well-characterized protein functional domains consisting of, from N- to C-terminus, signal sequence, pro-peptide, catalytic, O-glycosylation, and the hemopexin domains [19] (Figure 3A). The fibronectin type-II (FNII) repeat domain critical for substrate binding is contained within the catalytic domain. To gain a better understanding of the protein domains involved in the ssDNA enhancement of enzymatic activity, we examined the effect of ssDNA on the core catalytic domain (aa 107–449). The catalytic core domain-truncated protein showed catalytic activity without AMPA, as expected, since this protein is devoid of the shielding pro-peptide. ssDNA further enhances the enzymatic activity of the core domain protein in a concentration-dependent manner, indicating that the core domain encompasses the minimal structures required for the ssDNA modulation (Figure 3B). In fact, the increase in enzymatic activity for the core catalytic domain was much greater than that for the full-length protein. This observation was confirmed by selective deletion of the O-glycosylation or the hemopexin domains which also showed greater potentiation of the enzymatic activity by ssDNA (Figure 3C). Selective deletion of the FNII domains in the core catalytic domain within the background of otherwise full-length protein showed a graded reduction in the ssDNA-mediated increase in the enzymatic activity as more FNII domains were deleted. When all three FNII domains were deleted, ssDNA failed to increase the MMP9 enzymatic activity (Figure 3C). This loss of ssDNA potentiation in the domain-deleted proteins was not due to the inability of the substrate to bind to the catalytic domain since the deletion mutants maintained their ability to cleave the reporter substrate.

The likely significance of the FNII domain in ssDNA enhancement of MMP9 activity was further explored by examining its action on structurally related MMP2 (gelatinase) with an FNII domain, and MMP1 (collagenase) and MMP3 (stromelysin) without an FNII domain. The respective mCherry-tagged MMPs were overexpressed by transfection of HEK293 cells and the proper expression of the fusion protein was confirmed by Western blot (Figure 3D,E). The protein amount secreted into the cell culture media was quantified by measuring the direct mCherry fluorescence (Figure 3F) and MMP activity assay was performed on APMA pre-activated cell culture media with and without ssDNA. ssDNA enhanced MMP2 activity, while no enhancement was observed for MMP1 or MMP3 (Figure 3G), confirming the likely importance of the FNII domain.

We wanted to document enhanced MMP9 proteolytic activity by ssDNA in a more biological context. MMPs have been documented to play a significant role in axon guidance and growth [20,21] and MMP9 was reported to promote NGF-induced neurite outgrowth in PC12 cells [22]. We examined the effect of ssDNA on this well-described system. NGF stimulation induced neurite outgrowth and ssDNA applied to the cell culture medium-enhanced neurite outgrowth. Quantitative image analysis demonstrated no increase in the number of nuclei but an increase in neurite density and neurite density/cell (Figure 4A, i–iii). NGF treatment alone increased MMP9 activity in the culture supernatant and ssDNA further increased the activity (Figure 4A, iv). To clarify the precise role of MMP9 in NGF-induced neurite extension, we created a PC12 cell line where the MMP9 gene was deleted using the CRISPR–Cas9 (CRISPR-associated protein 9) system. Several guide RNA targeting the MMP9 gene was created, and PC12 cells were transfected with guide RNA and subjected to puromycin selection. Clonal expansion of cells expressing one of the guide RNA gave an MMP9-null PC12 line confirmed by direct sequencing of the intended target area of the MMP9 gene and enzymatic activity assay. Direct zymography of the cell line lysates confirmed much diminished gelatinolytic activity in the MMP9-null PC12 line (Supplementary Figure S5). Cells similarly selected after infection with a blank guide RNA (i.e. the same plasmid construct but without insertion of the guide RNA sequence) — expressing lentivirus created the sgBlank control PC12 cell line where the MMP9 gene remained intact to serve as a negative-control. The sgBlank PC12 cells demonstrated a NGF-induced increase in neurites/cell and ssDNA further enhanced this neurite extension as observed for wild-type PC12 cells. In MMP9-null PC12 cells, NGF only induced a minimal increase in neurite/cell count and ssDNA had no effect on this MMP9-independent effect of NGF

Biochemical Journal (2018) **475** 1597–1610
https://doi.org/10.1042/BCJ20180035

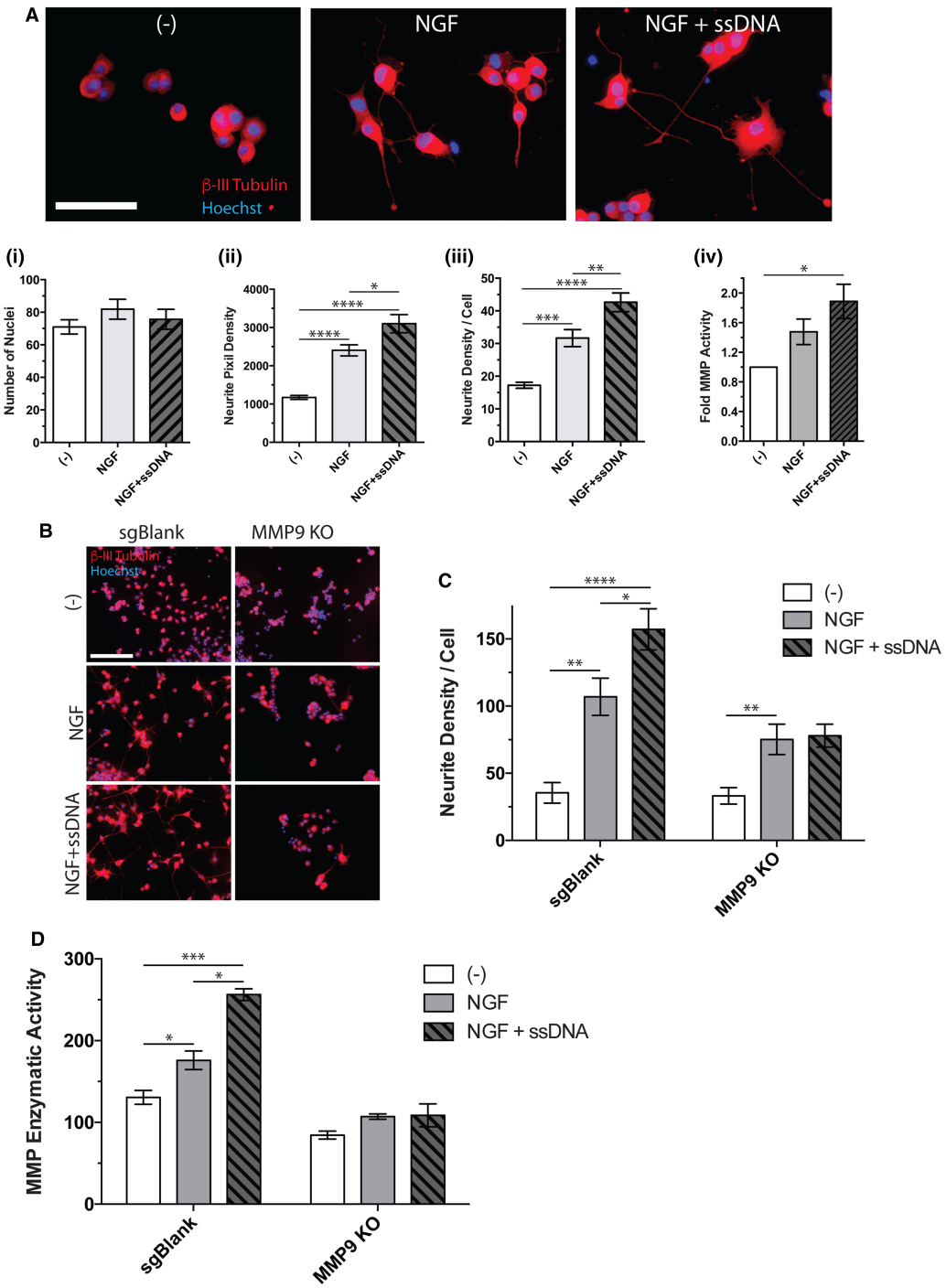

Figure 4. Oligonucleotide-induced enhanced PC12 neurite outgrowth.

(**A**) Immunofluorescent labeling of PC12 neurites in media only (left), NGF stimulation (middle), or NGF and ssDNA stimulation (left). β-III-Tubulin (red) was used to stain the cytoplasm and neurite extensions, while Hoechst stain (blue) was used for nuclear staining. Scale bar = 50 μm. (**A**i) Neurite Tracer software was used to quantify the number of nuclei and (**A**ii) the total cytoplasm/neurite density. (**A**iii) Neurite density per cell was calculated by normalizing the neurite density by total number of nuclei. (**A**iv) Prior to immunofluorescent labeling, culture medium was removed and MMP enzymatic activity was measured. (**B**) Immunofluorescent labeling of sgBlank control (left) and MMP9 KO PC12 cells (right) in media only (top), NGF stimulation (middle), or NGF and ssDNA stimulation (bottom) with Hoechst nuclear stain on the left, α-III-tubulin in the middle, and merged analysis on the right. Scale bar = 100 μm. (**C**) Neurite density per cell was calculated for each stimulation condition in wild-type (sgBlank) or MMP9 KO PC12 cells. (**D**) MMP enzymatic activity of conditioned media for each condition in wild-type (sgBlank) or MMP9 KO PC12 cells.

(Figure 4B,C). Culture media assayed for MMP9 activity in sgBlank cells demonstrated an increase in the catalytic activity by NGF with further enhancement by ssDNA as previously observed for the wild-type cells. Supernatant from the MMP9-null PC12 cells showed no increase by NGF and no effect of ssDNA was observed (Figure 4D). These experiments with MMP9-null cells indicated that ssDNA enhanced an MMP9-dependent increase in neurite density/cell measured within the biological context of NGF-induced neurite extension. The result also suggested that NGF exhibited a small MMP9-independent increase in neurite density/cell.

Discussion

We initiated this project hoping to identify an ssDNA aptamer capable of enhancing the MMP9 enzymatic activity. We arrived at a surprising conclusion that MMP9 binds not only to ssDNA but also to polynucleotides including RNA and dsDNA. Several methods, including a direct pull-down of ssDNA, electrophoretic mobility shift assay, fluorescent polarization, and SPR, all confirmed ssDNA binding to MMP9. The consequence of ssDNA binding to MMP9 was an increase in the catalytic activity of the enzyme demonstrated by a direct fluorescent substrate cleavage assay and by cleavage of the PARP substrate. Various truncation constructs of MMP9 localized the ssDNA effect to the core catalytic domain of the MMP9 protein and more specifically to the FNII repeat domain. Moreover, ssDNA by itself does not activate pro-MMP9 and the manifestation of modulation of enzymatic function required prior activation of pro-MMP9 by AMPA. Thus, ssDNA, and most probably polynucleotides in general, acts as true allosteric enhancers of MMP9 catalytic activity in contrast with the previously described gelatin increase in enzyme activity through allosteric acceleration of MMP9 or MMP2 activation [8]. Examination of MMP1 and MMP3 as representative of collagenase and stromelysin MMPs, respectively, without the FNII repeat domains demonstrated no activity enhancement by ssDNA, while MMP2 with a strong structural analogy to MMP9 showed the expected activity enhancement. However, protein domains other than the FNII repeat are likely to regulate the ssDNA enhancement of catalytic activity as suggested by the observation that greater increase in the activity was observed for the catalytic core and the C-terminal (i.e. tOG and tHmPx) deletion constructs (Figure 3B,C). Deciphering the mechanisms underlying this apparent 'shielding' of ssDNA potentiation of MMP9 activity will require further exploration.

Hu et al. [23] reported that 6xHis tagged proteins inhibited MMP9 activity by chelation of Zn^{++} required for the catalytic activity. Overexpressed and purified MMP9-mCherry protein used in some of our assays was 6xHis tagged introducing a potential confound in our experiments. Could ssDNA diminish the 6xHis chelation of Zn^{++} resulting in an apparent increase in MMP9 activity? Several observations argue against the potential role of 6xHis tag in our observation of ssDNA enhancement of MMP9 activity. First, both 6xHis tagged in-house purified MMP9 and non-tagged commercial full-length MMP9 and catalytic domain MMP9 demonstrated activity enhancement by ssDNA. Second, our MMP9 activity assay buffer contained added free Zn^{++} rendering chelation to the point of limiting the enzymatic activity unlikely.

All polynucleotides share the polyanionic property due to the negatively charged phosphate backbone of nucleic acids. Polyanion-binding proteins are abundantly present in cells and molecular modulation of various protein functions by polyanions including nucleic acids is well described in the literature [24–26]. We tested the polyanionic hypothesis of MMP9 modulation by testing other polyanionic molecules reported to modulate protein functions. However, none of the polyanionic molecules tested shared the ability to increase the MMP9 enzymatic activity compared with nucleic acids. The polyanionic molecules examined exist as polymers of various lengths and the commercially purchased polyanionic preparation exists as polymers of mixed length, raising the possibility that the size of the polymers could have limited the access of these charged molecules to the MMP9 surface pockets of positive charges. While this possibility cannot be excluded, sheared genomic DNA with size distribution spanning ~0.5–3 kb or even very large unsheared genomic DNA increased the MMP9 enzymatic activity, much like the shorter ssDNA, suggesting that the large size of the modulator ligand is not a limiting factor. On the other hand, 2-mer and single-free nucleotides failed to modulate the enzymatic activity. Since smaller 2-mer and single-free nucleotides should have greater access to surface pockets of positive charges on the MMP9 protein surface, this observation also supports the likelihood that charge neutralization by nucleic acids is not the mechanism of increased enzymatic activity.

Could the nucleotide modulation of MMP9 activity have any physiological relevance? We examined the effect of ssDNA on NGF-induced neurite extension in PC12 as one model of potential biological manifestation of the novel nucleotide–MMP9 interaction. If extracellularly applied ssDNA were to have a biological effect through modulation of MMP9 activity, this implies the presence of activated MMP9 in the culture media. On

Biochemical Journal (2018) **475** 1597–1610
https://doi.org/10.1042/BCJ20180035

first sight, this assumption appears to be at odds with the well-accepted notion that MMP9 is secreted in an inactive form. However, our neurite extension assay experiments are conducted in cultures 3–4 days after initiation of NGF stimulation with sufficient time for activation of the secreted inactive pro-MMP9 through well-documented mechanisms such as acidification, oxidation, and potential auto- and hetero-molecular proteolytic cleavage. Clarification of the role of MMP9 in neurite extension will require further experiments.

Not only MMP9 is identified as a secreted protein acting in the extracellular space with extracellular matrix protein as the substrate, but the protease is also identified in intracellular compartments including the cytosol and the nucleus [27–30] with many potential intracellular substrates [31]. These cellular compartments are shared by nucleotides, including the genomic DNA and transcribed RNA, prior to splicing in the nucleus, processed mRNA and other RNA species in the cytosol, and DNA released to the extracellular compartment during many processes of cell death including a form of innate immunity termed NETosis in neutrophils [32,33]. As such, MMP9 interaction with nucleic acids and the consequent increase in the enzymatic activity could occur in any cellular compartment where the two components coexist. While highly speculative, DNA release during NETosis in response to microbial infection could trigger increased MMP9 activity contributing to diseases, such as arthritis and vasculitis, where hyperactive MMP9 has been implicated in the pathogenesis. While direct binding of MMP9 and DNA has not been documented, MMP2/9 have been shown to be present in NETs (neutrophil extracellular traps) [34,35], adding credence to the speculation on the role of DNA–MMP9 interaction in NETs. In a more biological context, the clearance of cellular debris after cell death could be enhanced through breakdown of the extracellular matrix due to increased MMP activity by the DNA liberated from cells. A similar mechanism could encourage neurite elongation after neuronal injury not only by providing a path for the growing neurite by enhancing degradation of the extracellular matrix but also by directly increasing the MMP9 effect on NGF-induced neurite elongation as we have shown for PC12 cells. There are probably many more biological compartments where the gelatinase MMPs and nucleotides coexist; however, any potential pathobiological consequences of this novel interaction must be viewed in light of the fact that the interaction is not covalent and with an apparent dissociation constant in the micro-molar range.

We report nucleic acid as a novel allosteric enhancer of MMP9 enzymatic activity; however, the precise mechanism of nucleic acid enhancement of MMP9 enzymatic activity and the potential biological implication of this modulation need further investigation. We believe that the ability to increase the MMP9 enzymatic activity will open new avenues of research to further define the biological and pathophysiological role of this pleotropic molecule.

Abbreviations

APMA, aminophenylmercuric acetate; CRISPR, clustered regularly interspaced short palindromic repeats; DMEM, Dulbecco's Modification of Eagle's Medium; ds, double stranded; FBS, fetal bovine serum; FNII, fibronectin type-II; HEK293, human embryonic kidney 293; MMP, matrix metalloproteinase; NET, neutrophil extracellular traps; NGF, nerve growth factor; NM, N-terminal rat MMP9; NTA, nitrilotriacetic acid; PARP, poly-ADP-ribose-polymerase; PC12, pheochromocytoma 12; SELEX, systematic evolution of ligand by exponential enrichment; SPR, surface plasmon resonance; ssDNA, single-stranded DNA.

Author Contribution

T.D. and J.Y. designed the study and wrote the manuscript. T.D., X.C., R.W., and J.Y. performed experiments and analyzed data.

Funding

The present study was supported by RO1 GM105665 grant from the National Institutes of Health and the Bamforth Endowment Funds from the Department of Anesthesiology at UW Madison.

Competing Interests

The Authors declare that there are no competing interests associated with the manuscript.

References

1 Rohani, M.G. and Parks, W.C. (2015) Matrix remodeling by MMPs during wound repair. *Matrix Biol.* **44–46**, 113–121 https://doi.org/10.1016/j.matbio.2015.03.002

2 Iver, R.P., Jung, M. and Lindsey, M.L. (2016) MMP-9 signaling in the left ventricle following myocardial infarction. *Am. J. Physiol. Heart Circ. Physiol.* **311**, H190–H198 https://doi.org/10.1152/ajpheart.00243.2016
3 Dziembowska, M. and Wlodarczyk, J. (2012) MMP9: a novel function in synaptic plasticity. *Int. J. Biochem. Cell Biol.* **44**, 709–713 https://doi.org/10.1016/j.biocel.2012.01.023
4 Stawarski, M., Stefaniuk, M. and Wlodarczyk, J. (2014) Matrix metalloproteinase-9 involvement in the structural plasticity of dendritic spines. *Front. Neuroanat.* **8**, 68 https://doi.org/10.3389/fnana.2014.00068
5 Yamamoto, K., Murphy, G. and Troeberg, L. (2015) Extracellular regulation of metalloproteinases. *Matrix Biol.* **44–46C**, 255–263 https://doi.org/10.1016/j.matbio.2015.02.007
6 Emonard, H. and Hornebeck, W. (1997) Binding of 92 kDa and 72 kDa progelatinases to insoluble elastin modulates their proteolytic activation. *Biol. Chem.* **378**, 265–271 https://doi.org/10.1515/bchm.1997.378.3-4.265
7 Morgunova, E., Tuuttila, A., Bergmann, U., Isupov, M., Lindqvist, Y., Schneider, G. et al. (1999) Structure of human pro-matrix metalloproteinase-2: activation mechanism revealed. *Science* **284**, 1667–1670 https://doi.org/10.1126/science.284.5420.1667
8 Bannikov, G.A., Karelina, T.V., Collier, I.E., Marmer, B.L. and Goldberg, G.I. (2002) Substrate binding of gelatinase B induces its enzymatic activity in the presence of intact propeptide. *J. Biol. Chem.* **277**, 16022–16027 https://doi.org/10.1074/jbc.M110931200
9 Dupont, D.M., Andersen, L.M., Kotkjaer, K.A. and Andreasen, P.A. (2011) Nucleic acid aptamers against proteases. *Curr. Med. Chem.* **18**, 4139–4151 https://doi.org/10.2174/092986711797189556
10 Bock, L.C., Griffin, L.C., Latham, J.A., Vermaas, E.H. and Toole, J.J. (1992) Selection of single-stranded DNA molecules that bind and inhibit human thrombin. *Nature* **355**, 564–566 https://doi.org/10.1038/355564a0
11 Sela-Passwell, N., Rosenblum, G., Shoham, T. and Sagi, I. (2010) Structural and functional bases for allosteric control of MMP activities: can it pave the path for selective inhibition? *Biochim. Biophys. Acta, Mol. Cell Res.* **1803**, 29–38 https://doi.org/10.1016/j.bbamcr.2009.04.010
12 Duellman, T., Burnett, J. and Yang, J. (2015) Functional roles of N-linked glycosylation of human matrix metalloproteinase 9. *Traffic* **16**, 1108–1126 https://doi.org/10.1111/tra.12312
13 Duellman, T., Burnett, J. and Yang, J. (2015) Quantitation of secreted proteins using mCherry fusion constructs and a fluorescent microplate reader. *Anal. Biochem.* **473**, 34–40 https://doi.org/10.1016/j.ab.2014.12.010
14 Duellman, T., Warren, C.L., Peissig, P., Wynn, M. and Yang, J. (2012) Matrix metalloproteinase-9 genotype as a potential genetic marker for abdominal aortic aneurysm. *Circ. Cardiovasc. Genet.* **5**, 529–537 https://doi.org/10.1161/CIRCGENETICS.112.963082
15 Pool, M., Thiemann, J., Bar-Or, A. and Fournier, A.E. (2008) Neurite tracer: a novel ImageJ plugin for automated quantification of neurite outgrowth. *J. Neurosci. Methods* **168**, 134–139 https://doi.org/10.1016/j.jneumeth.2007.08.029
16 Murphy, M.B., Fuller, S.T., Richardson, P.M. and Doyle, S.A. (2003) An improved method for the in vitro evolution of aptamers and applications in protein detection and purification. *Nucleic Acids Res.* **31**, e110 https://doi.org/10.1093/nar/gng110
17 Yang, Y., Candelario-Jalil, E., Thompson, J.F., Cuadrado, E., Estrada, E.Y., Rosell, A. et al. (2010) Increased intranuclear matrix metalloproteinase activity in neurons interferes with oxidative DNA repair in focal cerebral ischemia. *J. Neurochem.* **112**, 134–149 https://doi.org/10.1111/j.1471-4159.2009.06433.x
18 Hill, J.W., Poddar, R., Thompson, J.F., Rosenberg, G.A. and Yang, Y. (2012) Intranuclear matrix metalloproteinases promote DNA damage and apoptosis induced by oxygen–glucose deprivation in neurons. *Neuroscience* **220**, 227–290 https://doi.org/10.1016/j.neuroscience.2012.06.019
19 Vandooren, J., Van den Steen, P.E. and Opdenakker, G. (2013) Biochemistry and molecular biology of gelatinase B or matrix metalloproteinase-9 (MMP-9): the next decade. *Crit. Rev. Biochem. Mol. Biol.* **48**, 222–272 https://doi.org/10.3109/10409238.2013.770819
20 Chang, C. and Werb, Z. (2001) The many faces of metalloproteases: cell growth, invasion, angiogenesis and metastasis. *Trends Cell Biol.* **11**, S37–S43 https://doi.org/10.1016/S0962-8924(01)82222-4
21 McFarlane, S. (2003) Metalloproteases: carving out a role in axon guidance. *Neuron* **37**, 559–562 https://doi.org/10.1016/S0896-6273(03)00089-8
22 Shubayev, V.I. and Myers, R.R. (2004) Matrix metalloproteinase-9 promotes nerve growth factor-induced neurite elongation but not new sprout formation *in vitro*. *J. Neurosci. Res.* **77**, 229–239 https://doi.org/10.1002/jnr.20160
23 Hu, J., Van den Steen, P.E., Houde, M., Ilenchuk, T.T. and Opdenakker, G. (2004) Inhibitors of gelatinase B/matrix metalloproteinase-9 activity: comparison of a peptidomimetic and polyhistidine with single-chain derivatives of a neutralizing monoclonal antibody. *Biochem. Pharm.* **67**, 1001–1009 https://doi.org/10.1016/j.bcp.2003.10.030
24 Salamat-Miller, N., Fang, J., Seidel, C.W., Assenov, Y., Albrecht, M. and Middaugh, C.R. (2007) A network-based analysis of polyanion-binding proteins utilizing human protein arrays. *J. Biol. Chem.* **282**, 10153–10163 https://doi.org/10.1074/jbc.M610957200
25 Urbinati, C., Chiodelli, P. and Musnati, M. (2008) Polyanionic drugs and viral oncogenesis: a novel approach to control infection, tumor-associated inflammation and angiogenesis. *Molecules* **13**, 2758–2785 https://doi.org/10.3390/molecules13112758
26 Song, E.S., Ozbil, M., Zhang, T., Sheetz, M., Lee, D., Tran, D. et al. (2015) An extended polyanion activation surface in insulin degrading enzyme. *PLoS ONE* **10**, e0133114. https://doi.org/10.1371/journal.pone.0133114
27 Fragkouli, A., Papatheodoropoulos, C., Georgopoulos, S., Stamatakis, A., Stylianopoulou, F., Tsilibary, E.C. et al. (2012) Enhanced neuronal plasticity and elevated endogenous sAPPα levels in mice over-expressing MMP9. *J. Neurochem.* **121**, 239–251 https://doi.org/10.1111/j.1471-4159.2011.07637.x
28 Pirici, D., Pirici, I., Mogoanta, L., Margaritescu, O., Tudorica, V., Margaritescu, C. et al. (2012) Matrix metalloproteinase-9 expression in the nuclear compartment of neurons and glial cells in aging and stroke. *Neuropathology* **32**, 492–504 https://doi.org/10.1111/j.1440-1789.2011.01279.x
29 Wiera, G., Wójtowicz, T., Lebida, K., Piotrowska, A., Drulis-Fajdasz, D., Gomułkiewicz, A. et al. (2012) Long term potentiation affects intracellular metalloproteinases activity in the mossy fiber — CA3 pathway. *Mol. Cell. Neurosci.* **50**, 147–159 https://doi.org/10.1016/j.mcn.2012.04.005
30 Mannello, F. and Medda, V. (2012) Nuclear localization of matrix metalloproteinases. *Prog. Histochem. Cytochem.* **47**, 27–58 https://doi.org/10.1016/j.proghi.2011.12.002
31 Cauwe, B. and Opdenakker, G. (2010) Intracellular substrate cleavage: a novel dimension in the biochemistry, biology and pathology of matrix metalloproteinases. *Crit. Rev. Biochem. Mol. Biol.* **45**, 351–423 https://doi.org/10.3109/10409238.2010.501783
32 Kaplan, M.J. and Radic, M. (2012) Neutrophil extracellular traps: double-edged swords of innate immunity. *J. Immunol.* **189**, 2689–2695 https://doi.org/10.4049/jimmunol.1201719

Biochemical Journal (2018) **475** 1597–1610
https://doi.org/10.1042/BCJ20180035

33 Jorgensen, I., Rayamajhi, M. and Miao, E.A. (2017) Programmed cell death as a defence against infection. *Nat. Rev. Immunol.* **17**, 151–164 https://doi.org/10.1038/nri.2016.147

34 Carmona-Rivera, C., Zhao, W., Yalavarthi, S. and Kaplan, M.J. (2015) Neutrophil extracellular traps induce endothelial dysfunction in systemic lupus erythematosus through the activation of matrix metalloproteinase-2. *Ann. Rheum. Dis.* **74**, 1417–1424 https://doi.org/10.1136/annrheumdis-2013-204837

35 Narasaraju, T., Yang, E., Samy, R.P., Ng, H.H., Poh, W.P., Liew, A.-A. et al. (2011) Excessive neutrophils and neutrophil extracellular traps contribute to acute lung injury of influenza pneumonitis. *Am. J. Pathol.* **179**, 199–210 https://doi.org/10.1016/j.ajpath.2011.03.013

36 Triebel, S., Bläser, J., Reinke, H. and Tschesche, H. (1992) A 25 kDa α_2-microglobulin-related protein is a component of the 125 kDa form of human gelatinase. *FEBS Lett.* **314**, 386–388 https://doi.org/10.1016/0014-5793(92)81511-J